ZnSTe coherently grown onto GaP substrates by molecular beam epitaxy using ZnS buffer layers

Kunio Ichino*, Shota Kashiyama, Nao Nanba, Hiroyasu Hasegawa, and Tomoki Abe

Department of Information and Electronics, Tottori University, Tottori, 680-8552, Japan

Received XXXX, revised XXXX, accepted XXXX
Published online XXXX

Key words: ZnSTe, GaP, ZnS-buffer, XRD-RSM, TEM

* Corresponding author: e-mail ichino@ele.tottori-u.ac.jp, Phone: +81-857-31-5240, Fax: +81-857-31-5240

$ZnS_{1-x}Te_x$ epitaxial layers with $x \sim 0.06$, nearly lattice-matched to GaP substrates, have been grown by molecular beam epitaxy. Direct growth of the layers onto the substrates results in poor crystal quality, showing no sign of coherent growth. This seems to be due to alloy composition deviation at the initial stage of the growth. To avoid the problem, a thin coherent ZnS buffer layer has been inserted at the ZnSTe/GaP interface. With the buffer layers, coherent growth of ZnSTe layers is achieved and the crystal quality has been improved.

1 Introduction ZnS has been known as efficient phosphors for cathode-ray tubes as well as a wide bandgap semiconductor, and thus considered as a possible material for semiconductor visible/UV light emitting devices [1]. It has also been known, however, that achieving p-type conduction in ZnS is very difficult. We have previously reported p-type conduction in $ZnS_{1-x}Te_x$:N layers in the range of $0.1 < x < 0.3$, and the operation of pn-junction light-emitting diodes [2,3]. The properties of the p-type layers, however, were not satisfactory for practical applications; e.g., the typical resistivity of $\sim 100\Omega$cm was not low enough and the photoluminescence intensity was very weak. For the improvement, one of the problems seems to be insufficient crystal quality of the $ZnS_{1-x}Te_x$ layers. Since these $ZnS_{1-x}Te_x$:N layers were grown on thick ZnS layers, a lattice-mismatch between $ZnS_{1-x}Te_x$ and ZnS (e.g., 1.9% for $x = 0.15$) seems to cause deterioration of the crystals.

$ZnS_{1-x}Te_x$ can be lattice-matched to GaP at a Te content x of 0.06, and superior crystal quality is expected if lattice-matched layers are grown on GaP substrates. Therefore, it is worthwhile to do p-type doping experiments on such layers. To date, epitaxial growth of ZnSTe has been reported by several groups, and most of them used GaAs as a substrate [4–6]. There have been only a limited number of reports on the growth on GaP substrates [7,8], and the details about crystallographic characterizations, concerning coherent growth or lattice-matching to the substrates, have not been reported. Therefore, we have studied the possibility of lattice-matching of ZnSTe to GaP substrates.

In this paper, we report the growth of $ZnS_{1-x}Te_x$ layers onto GaP substrates by molecular beam epitaxy (MBE). In particular, coherent growth of the $ZnS_{1-x}Te_x$ layer is achieved by using a thin ZnS buffer layer, accompanied by the improvement in the crystal quality.

2 Experiment Samples were grown by a MBE system designed for sulfide growth [9,10] using metal Zn and Te (Osaka Asahi Metal), and elemental S (Furukawa Denshi) as source materials. Since Te is less preferably incorporated into the film than S, the S beam flux was reduced for the growth of ZnSTe; specifically, the evaporation temperature of S was decreased from 155°C to 110°C. Under this condition, the Te content was controlled by changing Te beam flux. The average Te content of the layer was determined from the angle of the 004 X-ray diffraction (XRD) peak, assuming Vegard's law using lattice constants a_{ZnS}=5.4093Å and a_{ZnTe}=6.1026Å.

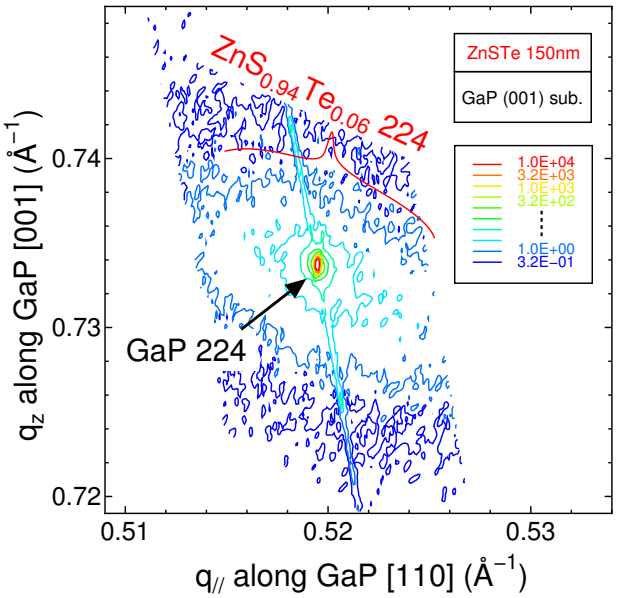

Figure 1 XRD RSM of $ZnS_{0.94}Te_{0.06}$ (150 nm) / GaP structure near 224 diffraction peaks. $q_{//}$ and q_z axes are reciprocal space coordinates along GaP [110] and [001] direction, respectively. Each line is a contour for the diffraction intensity. The peak for $ZnS_{0.94}Te_{0.06}$ spreads widely.

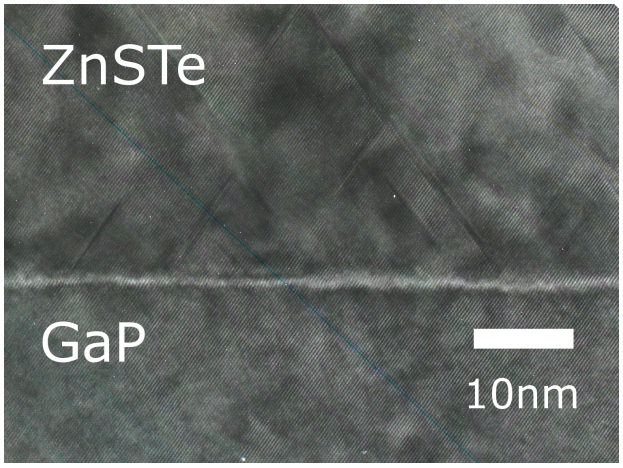

Figure 2 Cross-sectional TEM image of $ZnS_{0.94}Te_{0.06}$/GaP interface. At the interface, the lattice is distorted and many stacking faults arise.

For layers coherently grown to GaP substrates, the elastic strain is also considered using elastic stiffness constants $C_{11} = 10.46 \times 10^{10}$ N/m^2 and $C_{12} = 6.53 \times 10^{10}$ N/m^2 for ZnS, and $C_{11} = 7.13 \times 10^{10}$ N/m^2 and $C_{12} = 4.07 \times 10^{10}$ N/m^2 for ZnTe. As a substrate, an unintentionally doped n-type (001) GaP substrate (Shin-Etsu Handotai) was used. The layers were characterized by high-resolution X-ray diffraction (HRXRD) and transmission electron microscopy (TEM) using Rigaku SmartLab and JEOL JEM-2010, respectively. In the HRXRD measurement, reciprocal space maps (RSMs) around 224 reciprocal lattice points of $ZnS_{1-x}Te_x$ and GaP were measured using a Ge-(400) double-crystal monochromator and a 1-dimensional semiconductor array detector (D/teX Ultra). The layers were cut and thinned by lapping and Ar-ion milling for cross-sectional TEM observation. TEM images of the samples were recorded under the condition with an acceleration voltage of 200 kV and an electron beam parallel to [110] direction of the samples.

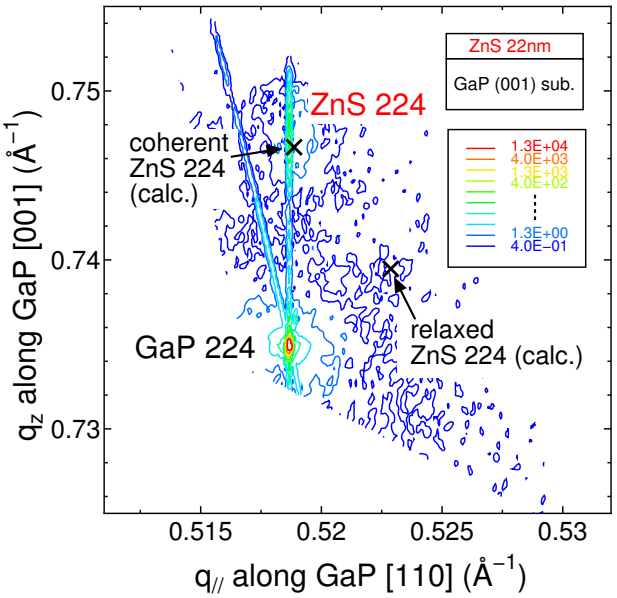

Figure 3 XRD RSM of ZnS (22 nm) / GaP structure. Each cross mark represents the calculated peak position of a coherently-grown ZnS layer or a relaxed ZnS layer (with the bulk lattice constant). The ZnS layer is coherent to GaP substrate. Since the epitaxial layer is ZnS, there is no peak in the bottom and left area below the GaP peak, which is outside of the measurement range.

3 Results and discussion First, $ZnS_{1-x}Te_x$ layers were directly grown onto GaP substrates. Figure 1 shows a XRD RSM of a $ZnS_{0.94}Te_{0.06}$ layer around 224 diffraction peaks. The horizontal and vertical axes represent the reciprocal space coordinates $q_{//}$ along GaP [110] and q_z along GaP [001], respectively. Accordingly, for a 224 peak, $q_{//}$ and q_z correspond to the reciprocals of the spacing of (220) and (004) lattice planes, respectively. In Fig. 1, the ZnSTe 224 peak spreads widely around the GaP 224 peak, indicating large variation in the spacing and the direction of the lattice planes in the ZnSTe layer. Although the layer has a Te content of $x = 0.06$, corresponding to the lattice-matching condition, the RSM shows no sign of coherent growth of the layer to the substrate, suggesting poor crystal quality.

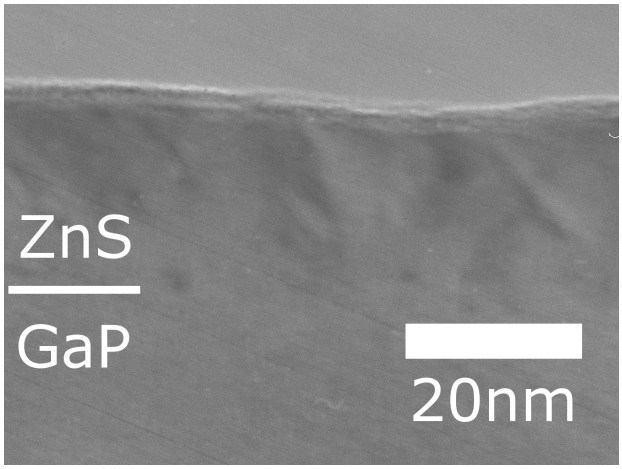

Figure 4 Cross-sectional TEM image of ZnS/GaP structure. No distinct defects are seen.

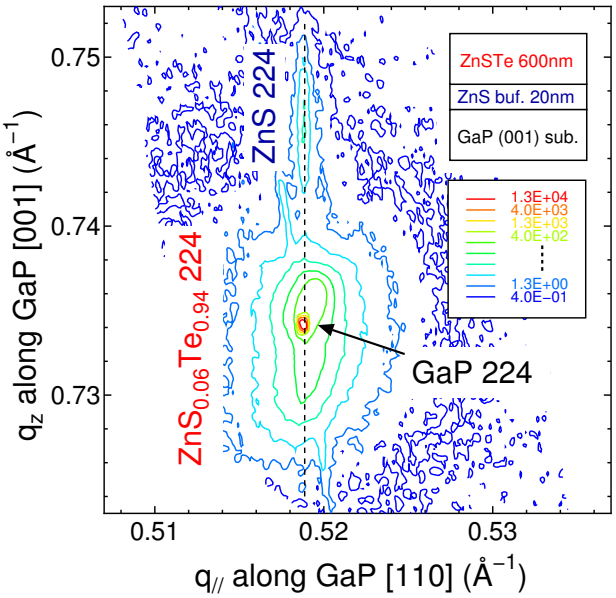

Figure 5 XRD RSM of $ZnS_{0.94}Te_{0.06}$ (600 nm) / ZnS (20 nm) / GaP structure. The $ZnS_{0.94}Te_{0.06}$ is also coherent to GaP substrate.

Figure 2 shows a cross-sectional TEM image of the same $ZnS_{0.94}Te_{0.06}$ sample. A large number of stacking faults arise from the ZnSTe/GaP interface and elongate to the ZnSTe layer. At least one of the reasons for the poor crystal quality, as revealed by the RSM measurement, seems to be the existence of these stacking faults. In addition, it can be seen that the lattice is largely distorted at the interface. From these facts, it is possible that the origin of the stacking faults is the deviation of the Te content in the initial stage of the growth, i.e., the growth on the GaP surface; the Te incorporation ratio seems to depend on the underlying materials and could be different on GaP from the value in succeeding growth.

In order to avoid this problem, a thin ZnS buffer layer was inserted between a $ZnS_{1-x}Te_x$ layer and a GaP substrate, with the idea that the chemical nature of ZnS seems to be similar to that of $ZnS_{1-x}Te_x$, especially for small x, and thus the Te content deviation should be suppressed. The ZnS buffer layer must be thinner than the critical thickness to avoid the generation of misfit dislocations since there is a lattice-mismatch of 0.77% between ZnS (a = 5.4093 Å) and GaP (a = 5.4512 Å). We previously reported that the critical thickness of a ZnS layer on a GaP substrate is less than 30nm [11]. To examine the suitability as a buffer layer, a thin ZnS layer was grown on a GaP substrate. Figure 3 shows a XRD RSM of a ZnS (22nm) / GaP structure, for an area around 224 diffraction peaks. The ZnS 224 peak is on the same $q_{//}$ coordinate as the GaP peak, showing coherent growth. The q_z coordinate of the ZnS peak shifts to a larger value from the bulk value owing to the 2-dimensional tensile strain and the resultant reduction of the (004) spacing. In addition, the ZnS 224 peak elongates along q_z axis because of its thinness; the peak width is given as $\Delta q_z \sim t^{-1}$ where t is the layer thickness.

A cross-sectional TEM image of the same sample is shown in Fig. 4. There are no distinct defects seen in Fig. 4, in contrast to Fig. 2, reflecting the fact that the ZnS layer thickness is below the critical thickness. As shown above, a thin ZnS layer below the critical thickness exhibits high crystal quality and thus it was used as a buffer layer for $ZnS_{1-x}Te_x$ growth in order to improve the crystal quality.

Figure 5 shows a 224 XRD RSM of a $ZnS_{0.94}Te_{0.06}$ (600 nm) / ZnS (20 nm) / GaP structure. The peak of the coherent ZnS layer is similar to the one shown in Fig. 3. In addition, it should be noted that the peak of ZnSTe is on the same $q_{//}$ coordinate as the GaP peak, indicating coherent growth. In comparison with Fig. 1, the crystal quality is much improved and thus the effect of the ZnS buffer layer is distinctly shown. Figure 6 shows the vertical sections of RSMs shown in Figs. 1, 3 and 5 at $q_{//} \sim 0.519$ where a GaP 224 peak is located. Note that the ZnSTe layer on a ZnS buffer layer exhibits much stronger peak than the ZnSTe layer directly grown on a GaP substrate. Concerning the shape of the ZnSTe peak in Fig. 5, it elongates along q_z axis, which appears to be similar to the ZnS peak. However, it is not due to the thinness since the ZnSTe layer is 600-nm thick and the peak width should be much smaller. The width along q_z axis is probably due to the slight change in Te content during the growth for some reason (a change in the effusion cell temperature, etc.), and slight partial deviation of $q_{//}$ from the GaP value may be caused by partial lattice-relaxation in the later part of the growth as a result of the composition change.

Figure 7 shows a cross-sectional TEM image of the same sample as for Fig. 5. Although some defects like

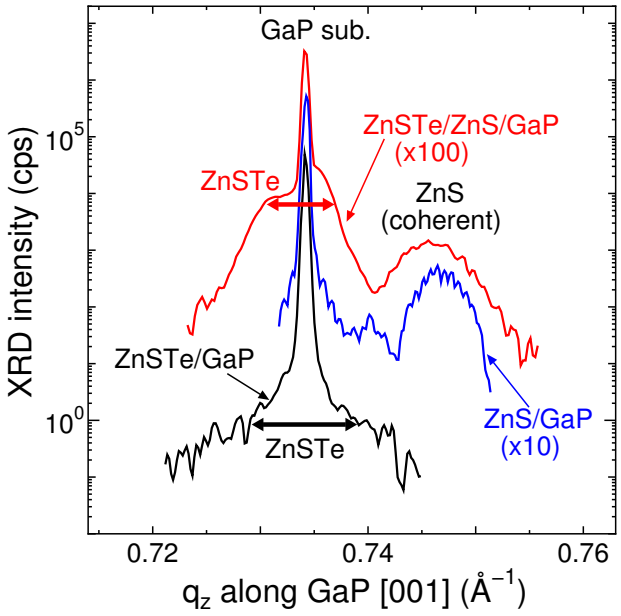

Figure 6 Vertical sections of RSMs shown in Figs. 1, 3 and 5 at $q_{//}$ ∼0.519 Å^{-1} where a GaP 224 peak is located.

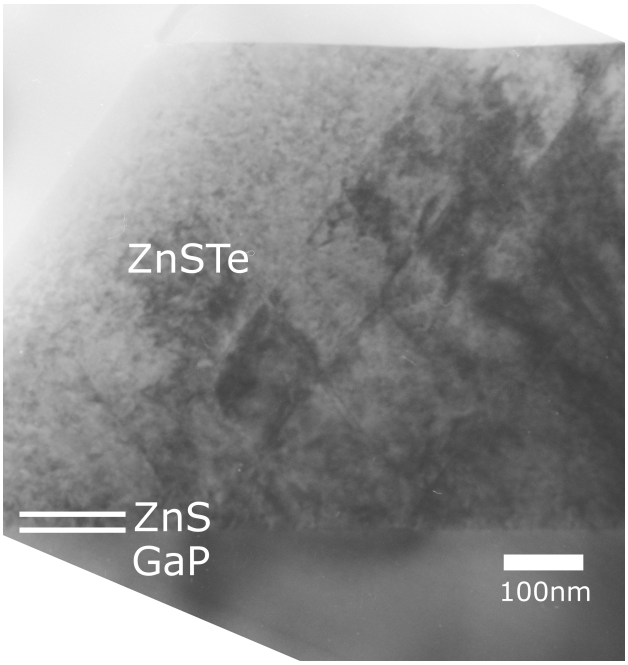

Figure 7 Cross-sectional TEM image of $ZnS_{0.94}Te_{0.06}$/ZnS/GaP structure. The defect density is reduced as compared to Fig. 2. Note the difference in the scale.

stacking faults are still seen, they are not concentrated at the epilayer/substrate interface and the density is much less than that in Fig. 2. (Here, note that the scales are different). Therefore, the generation of the defects at the interface is reduced by the insertion of the coherent ZnS buffer layer, probably owing to the suppression of the composition deviation at the initial growth stage. The defects still seen in Fig. 7 seem to be related to the partial lattice-relaxation due to the slight composition change discussed above. Thus it is thought that coherent growth was maintained during most part of the growth duration, and it is expected that the suppression of the unintentional composition change during the growth leads to the perfect lattice-match between ZnSTe and GaP.

4 Conclusions $ZnS_{1-x}Te_x$ epitaxial layers have been grown on (001) GaP substrates by MBE. Direct growth of the layers onto the substrates results in poor crystal quality even for $x \sim 0.06$ corresponding to the lattice-matching condition, showing no sign of coherent growth. By inserting a thin (∼ 20 nm) coherent ZnS buffer layer at the $ZnS_{0.94}Te_{0.06}$/GaP interface, coherent growth of the ZnSTe layer to the GaP substrate is realized and the crystal quality is also improved. The effect of the buffer layer seems to be the suppression of the alloy composition deviation and resultant defect formation at the initial stage of the growth.

Acknowledgements This work was supported by JSPS KAKENHI Grant Number 26390053.

References

[1] S. Shionoya, in: Phosphor Handbook, edited by S. Shionoya and W. M. Yen, (CRC Press, Boca Raton, 1999) Chap. 3, Sec. 2.
[2] K. Ichino, T. Kojima, S. Obata, T. Kuroyanagi, S. Nakazawa, and S. Kashiyama, Appl. Phys. Express, **6**, 112102 (2013).
[3] K. Ichino, T. Kojima, S. Obata, T. Kuroyanagi, K. Kimata, S. Nakazawa, and S. Kashiyama, Phys. Status Solidi C **11**, 1282 (2014).
[4] I. K. Sou, K. S. Wong, Z. Y. Yang, H. Wang, and G. K. L. Wong, Appl. Phys. Lett. **66**, 1915 (1995).
[5] M. Kobayashi, C. Setiagung, K. Wakao, S. Nakamura, A. Yoshikawa, and K. Takahashi, J. Cryst. Growth **184/185**, 66 (1998).
[6] Y.-M. Yu, S. Nam, J.-K. Rhee, B. O, K.-S. Lee, and Y. D. Choi, J. Cryst. Growth **210**, 521 (2000).
[7] I. K. Sou, C. L. Man, Z. H. Ma, Z. Yang, and G. K. L. Wong, Appl. Phys. Lett. **71**, 3847 (1997).
[8] Z. H. Ma, I. K. Sou, K. S. Wong, Z. Yang, and G. K. L. Wong, Appl. Phys. Lett. **73**, 2251 (1998).
[9] K. Ichino, K. Ueyama, M. Yamamoto, H. Kariya, H. Miyata, H. Misasa, M. Kitagawa, and H. Kobayashi, J. Appl. Phys. **87**, 4249 (2000).
[10] K. Ichino, T. Nishikawa, F. Kawakami, T. Kosugi, M. Kitagawa, and H. Kobayashi, Phys. Status Solidi B **229**, 217 (2002).
[11] K. Ichino, A. Nishigaki, and A. Yamauchi, Phys. Status Solidi C **9**, 1744 (2012).